Arabian Journal of Chemistry (2020) 13, 6589–6597

King Saud University

Arabian Journal of Chemistry

www.ksu.edu.sa
www.sciencedirect.com

ORIGINAL ARTICLE

Anti-obesity activity of gold nanoparticles synthesized from *Salacia chinensis* modulates the biochemical alterations in high-fat diet-induced obese rat model via AMPK signaling pathway

Lei Gao [a,1], Yangxi Hu [a,1], Desheng Hu [a], Ying Li [a], Songpeng Yang [a], Xing Dong [a], Sulaiman Ali Alharbi [b], Hansong Liu [a,*]

[a] *Department of Gastrointestinal Hernia Surgery, Zhengzhou Central Hospital Affiliated to Zhengzhou University, Zhengzhou City, Henan Province 450002, China*
[b] *Department of Botany and Microbiology, College of Science, King Saud University, Riyadh 11451, Saudi Arabia*

Received 27 April 2020; accepted 12 June 2020
Available online 24 June 2020

KEYWORDS

Gold nanoparticles;
Salacia chinensis;
Obesity;
High-fat diet;
AMPK signaling

Abstract *Salacia chinensis* (SC) is generally known as Saptrangi, which has been used as an herb in Ayurvedic medicine and has a broad range of biological applications. The current research was planned to develop *Salacia chinensis*-loaded gold nanoparticles (SC-AuNPs) and to assess the anti-obesity parameters in a high-fat diet (HFD) treated obese rats. SC-AuNPs were synthesized and characterized using UV–visible spectroscopy, SEM, FTIR, EDX, XRD, and TEM. Furthermore, the bodyweight changes, BMI, adipose index, leptin, resistin, adiponectin, AI, CRI, liver marker enzymes, inflammatory markers, lipid profile, AMPK signaling proteins, and liver histopathological changes were analyzed. We observed that the synthesized SC-AuNPs had a spherical shape, crystalline nature, and possessed a different functional group. The SC-AuNPs treatments also decreased body weight, BMI, adipose index, leptin, resistin, AI, CRI, liver marker enzymes, lipid profile, inflammatory markers, and AMPKα1. On the other hand, SC-AuNPs treatment increased adiponectin, HDL-C, and pAMPKα1. The histopathological findings showed improved result with reduced hepatocyte degradation under the influence of SC-AuNPs treatment.

* Corresponding author.
E-mail address: 13613837150@sina.cn (H. Liu).
[1] Equal contribution.

Peer review under responsibility of King Saud University.

Production and hosting by Elsevier

1. Introduction

Obesity is a long-term metabolic disorder, which is described by a severe accumulation of body fat and abnormal metabolism of lipids. Hyperlipidemia is effectively related to long-term diseases including cardiovascular diseases, type 2 diabetes, respiratory complications, and cancer (Kopelman,

https://doi.org/10.1016/j.arabjc.2020.06.015
1878-5352

2000). In modern days, obesity has been augmented surprisingly to 800% worldwide, which necessitates for the weight-reducing surgery methods which control such metabolic disorders (Chen et al., 2018). Cellular cholesterol homeostasis indicates a balance between many complex and interactive processes. This involves uptake of extracellular cholesterol through the LDL receptor signaling, intracellular cholesterol trafficking, cholesterol esterification/deacylation reactions, de novo cholesterol synthesis, and cellular efflux (Brown and Goldstein, 1983). Thus, there remains an imperative and emergent necessity for efficient approaches in response to the overall obesity pandemic.

Here, our current interest lies in the fact that nanoparticle (NP) may provide us a novel beneficial mediator in the control and cure of obesity. Nanotechnology indicates to the chemical and physical production of substances having nanosize among 1–100 nm (Jeevanandam et al., 2018). Numerous nanomaterials being improved for nanomedicine usages, particularly AuNPs are referred to as potentially used in the medical field and it efficiently increases the drug delivery system. AuNPs are mostly stable metals NPs and have interesting possessions likes size associated biocompatibility, magnetism, nontoxic nature, and electronic materials (Arvizo et al., 2010). AMPK takes an essential function on the energy balance of the body, prevents the synthesis of fatty acid, and stimulates the fatty acid oxidation (Kemp et al., 2003). The AMPK can induce metabolic changes, which involve both chronic effects in the expression status of the genes and acute effects in the phosphorylation of key enzymes implicated for metabolic regulation (Kola et al., 2008). Therefore, AMPK has been considered as a hopeful goal for the management of hyperlipidemia and obesity.

Natural plants have been verified to have a dual effect, acting both as capping and reducing agent, thus improving the pharmacological effectiveness and constancy of AuNPs (Benedec et al., 2018). The plant-based synthesis of metallic NPS is a growing marketable requirement due to its broad applicability in different fields such as chemistry, medicine, energy, catalysis, electronics, and cosmetics. Numerous previous studies have reported the anti-obesity and antioxidant properties of biogenic AuNPs on animal models (Chen et al., 2018; Chen et al., 2018; Yi et al., 2020). *Salacia chinensis* (SC) is generally known as Saptrangi, which has been used as an herb in Ayurvedic medicine (Deokate and Khadabadi, 2012). This plant is widely distributed in South-East Asia and Australoceania. The plant extract demonstrates different pharmacological activities such as antihyperglycemic, anticaries, antioxidant, antiulcer, antidiabetic, antiobesity, anticancer, hepatoprotective, and skin lightening agents (Yoshikawa et al., 2003; Sellamuthu et al., 2009; Tran et al., 2008; Asuti, 2010). In the present study, we have been using an extract of *Salacia chinensis* for the bio-fabrication of AuNPs and explored their anti-obesity properties.

2. Materials and methods

2.1. Chemicals

Gold(III) chloride trihydrate ($HAuCl_3$) (99.9% pure) was attained from Sigma-Aldrich (St.Louis, MO, USA). Primary antibodies for pAMPKα1, AMPKα1, and β-actin were procured from Santa-Cruz Biotechnology (Santa-Cruz, CA). ELISA kits for TNF-α and IL-1β were procured from R&D Systems Inc, (Minneapolis, MN). Reagent kits for TG, FFA, TC, and HDL-C were obtained from Abcam, USA.

2.2. Experimental animals

A total of 30 male albino Wistar animals 7–8 weeks old were obtained and used in the current work. Each rat weighed approximately 180–210 g. All the experiments were approved by institutional ethical committee Zhengzhou Central Hospital Affiliated to Zhengzhou University, Zhengzhou City, Henan Province, 450002, China. They were accommodated in an animal house and maintained at room temperature (24 ± 2 °C) under the controlled environmental condition of 12 h light/12 h dark cycle. All rats were given with regular rat pellet food along with water *ad libitum*.

2.3. Preparation of High-fat diet

For each 100 g of rat food, 68 g of the regular powder form of rat chow was combined with 32 g of ghee, the procedure was modified from NikNorliza et al. (NikNorliza et al., 2014; NikNorliza et al., 2014). A high-fat diet (HFD) was combined along with calcium (300 mg) and vitamin D3 (100 IU). The combination was mixed with marble-shaped dough samples and incubated at −40 °C until it got thickened.

2.4. Experimental design and stimulation of obesity

The group-1 rats were fed with the standard pellet food during the experiments. All other rats were fed with an HFD consisting of 42% fat content for six weeks before allocating them to various treatment groups. Group-2 rats were fed with HFD and no other treatment. Group-3 rats were fed HFD with 10 mg/kg bwt of SC-AuNPs, group-4 with HFD with 20 mg/kg bwt of SC-AuNPs, and group-5: HFD with 30 mg/kg bwt of SC-AuNPs for six weeks by orally. Bodyweight of all rats was documented weekly and alterations on bodyweight were measured carefully. After animal sacrifice, the blood samples were gathered in heparinized containers, and plasma extracted for different biochemical estimations.

2.5. Preparation of SC leaf extract

The fresh SC leaves were collected, washed and shadow dried until the water fully dried. 10 g of powdered plant sample was heated along with 100 ml of double distilled water for 10 min, sieved through Whatmann no. 1 filter paper, and used for the synthesis of AuNPs.

2.6. Synthesis of SC-AuNPs

The SC-AuNPs were biosynthesized by adding 45 ml of 1 mM $HAuCl_3$ solution and 5 ml of SC aqueous leaf extract to reduce the Au^{3+} ions to Au^0. The reaction mixture was placed in the orbital shaker at 30 °C. The formation of SC-AuNPs was identified through the change in the color of the sample from yellow to ruby red (Elia et al., 2014). The AuNPs were pelleted from the reaction solution by centrifuging at 10,000 rpm for

15 mins. The supernatant was discarded and AuNPs were collected and placed in the oven for 2 h for drying at 40 °C. The dried SC-AuNPs pellets were utilized for the different characterization techniques and further *in vivo* studies.

2.7. Characterization of SC-AuNPs

The production of SC-AuNPs was established by UV spectral investigation. The spectral absorbance was verified by UV spectroscopy at a wavelength range from 200 to 800 nm. The size and surface morphology of the SC-AuNPs was observed via SEM, TEM, and EDX on the NOVA-450 instrument. FTIR was carried out in Thermo-Scientific™ Nicolet-iS™50 FTIR spectrometer for identifying the promising biomolecules of the synthesized SC-AuNPs. The crystalline nature of the synthesized SC-AuNPs was analyzed by the XRD technique using the Shimadzu XRD-6000/6100 model. The XRD study was carried out using Cu-Kα radiation within the range of $2\theta = 10–70°$.

2.8. Determination of BMI, adipose index, leptin, resistin, and adiponectin

The BMI and adipose index was measured by using the formulas: BMI = body weight (g)/length^2 (cm^2); adipose index (%) = retroperitoneal, whole weight of the visceral and epididymal fat/final bodyweight. Leptin, resistin, and adiponectin were determined using the ELISA method.

2.9. Liver marker enzymes

The levels of plasma liver marker enzymes such acid-phosphatase (ACP) and alkaline-phosphatase (ALP) status were investigated following the protocol of King (King, 1965; King, 1965) as explained by Balasubramanian et al. (Balasubramanian et al., 1983; Balasubramanian et al., 1983). Alanine-transaminase (ALT) and aspartate-transaminase (AST) status were evaluated as reported by Bergmeyer et al. (Bergmeyer et al., 1978; Bergmeyer et al., 1978).

2.10. Lipid profile, atherogenic index, and coronary risk index

The levels of plasma lipid profile such as FFA, TC, TG, and HDL-C was determined with a commercial kit. The levels of VLDL-C and LDL-C were measured and derived using the formula, VLDL-C = TG/5, and LDL-C = TC − (HDL-C + VLDL-C).

2.11. Measurement of inflammatory mediators

The level of plasma inflammatory mediators i.e. interleukin-1beta (IL-1β) and tumor necrosis factor-alpha (TNF-α) was estimated with the aid of ELISA kit following the manufacturer's instructions.

2.12. Histopathological analysis

The liver tissues from experimental rats were sectioned, treated with formalin (10%), and dehydrated with ethanol solutions (50–100%). The sections of the 3–5 μm range were incised, stained with hematoxylin and eosin (H&E), and investigated using the optical microscope.

2.13. Western blotting analysis

The liver tissue was homogenized and centrifuged at 12,000 rpm (4 °C) for 15 min. After this, the upper aqueous phase was collected and proteins were quantified using Lowry's method (1951) (Lowry et al., 1951). Proteins were separated using an SDS-PAGE and the protein expression was determined using the primary antibodies of pAMPKα1 and AMPKα1. The bands were observed using enhanced chemiluminescence reagent kits and the intensity of the band was determined by ImageJ software.

2.14. Statistical analysis

The statistical examination was employed by using the SPSS 16 statistical package. The data were characterized as mean ± SD. One way ANOVA and DMRT measurement was used to compare the difference between the variable groups. The differences were considered significant at $p < 0.05$.

3. Results

3.1. Characterization of SC-AuNPs

Fig. 1 demonstrates the UV–vis spectra of bio-fabricated SC-AuNPs. The steadiness of bio-fabricated SC-AuNPs was concluded based on the highest absorbance peak and the alterations of color from yellow to ruby red.

Fig. 2A and B show the morphological changes of SEM and TEM analysis. The electron microscopical images of SC-AuNPs showed the size and shape of nanoparticles as a function of the extract that measured ranging from 20 to 50 nm.

Fig. 2C shows the EDX spectra of SC-AuNPs. The EDX investigation of a stabilized SC-AuNPs as well as showed the existence of AuNPs stabilized via plant biomolecules. In the present study, applicable spectra with powerful signals of Au at the characteristic wavelength were observed.

Fig. 3 reveals the crystalline nature of the synthesized SC-AuNPs as identified using the XRD investigation. The XRD patterns showed numerous Bragg reflections that could be classified according to the FCC formation of gold. Diffraction peaks were identified at $2\theta = 100$ (31.94°), 002 (33.67°), 101 (36.84°), 102 (47.86°), 110 (57.34°) and 103 (62.64°) to confirm the presence of gold ions. Thus, the XRD patterns revealed that the SC-AuNPs were crystalline.

Fig. 4 demonstrates the FTIR spectra of the SC extracts and its binding capacity to the AuNPs. FTIR spectra established the existence of different active molecules. For instance, the peaks were observed at 3268.91 (alcohols O—H stretch), 3008.75 (carboxyl acids O—H stretch), 2920.95 (carboxyl acids O—H stretch), 2853.24 (carboxyl acids O—H stretch), 1708.03 (ketone C═O stretch), 1621.17 (alkenyl C═C stretch), 1406.27 (alkanes C—C stretch), 1245.12 (alkyl ketone C═O Stretch), 1144.09 (aliphatic stretch C—O), 1076.47 (primary alcohol C—O stretch), 997.08 (alkene C═C bend), 855.90 (halo compound C-Cl), 758.00 (alkene C═C bend), 703.15

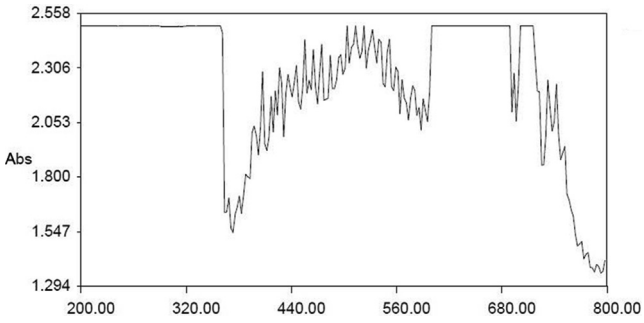

Fig. 1 UV–vis spectral analysis of AuNPs synthesized from SC.

(aromatic compounds) and 532.82 (halogen compound) for the SC-AuNPs.

3.2. Effect of SC-AuNPs on body weight and BMI of control and obese rats

The HFD supplemented rats revealed a considerable ($p < 0.05$) augment on the body weight as well as BMI evaluated to control rats. The obese animals treated with different dosages (10, 20, and 30 mg/kg body weight) of SC-AuNPs illustrated a decrease ($p < 0.05$) in BMI and body weight compared to the untreated obese animals as shown in Table 1.

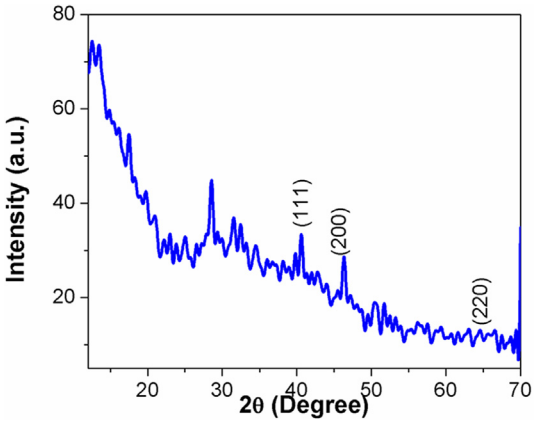

Fig. 3 XRD pattern of AuNPs synthesized from SC.

3.3. Effects of SC-AuNPs on leptin, adipose index, resistin and adiponectin of control and obese rats

The adipose index, leptin, and resistin of control obese rats were notably ($p < 0.05$) high, whereas adiponectin considerably ($p < 0.05$) diminished when compared to the control animals. Interestingly, SC-AuNPs (10, 20, and 30 mg/kg body weight) treated groups of HFD induced rats revealed a

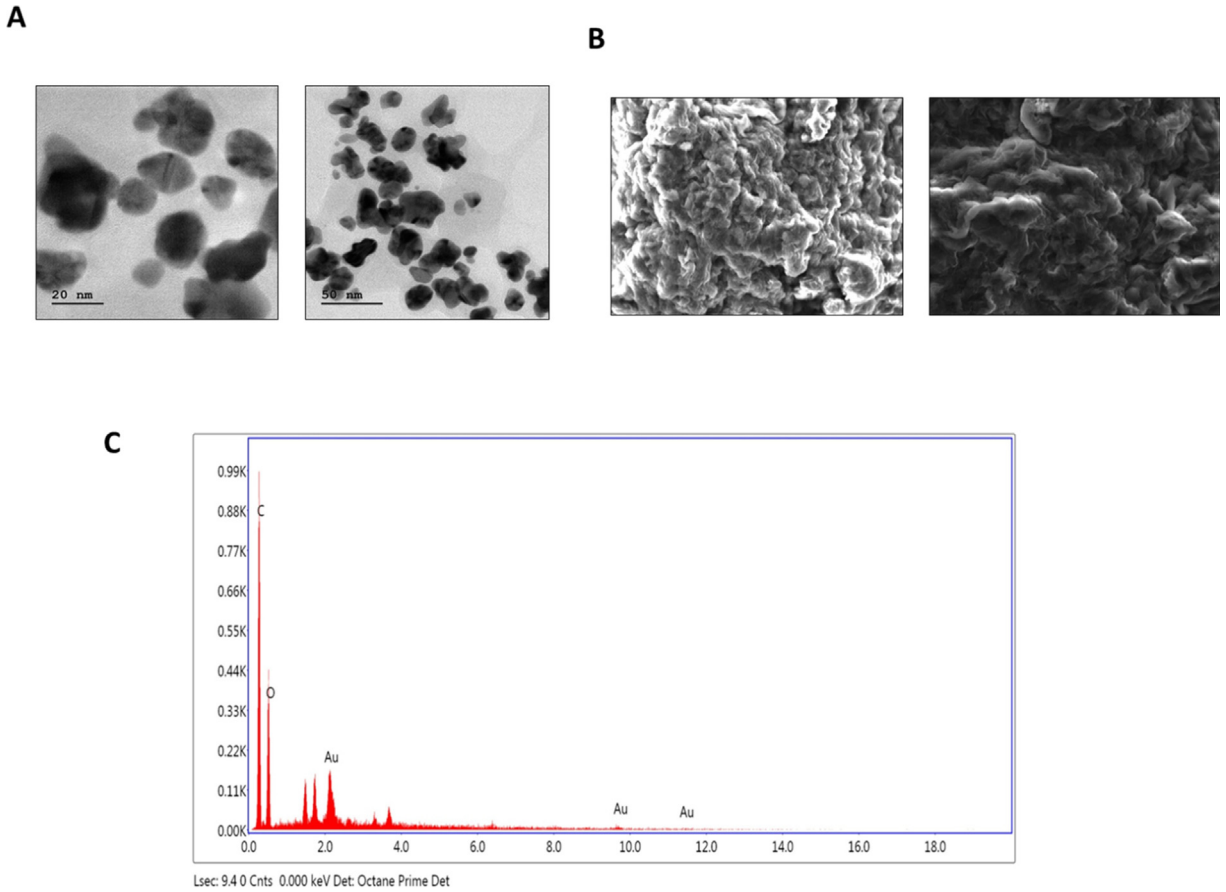

Fig. 2 TEM, SEM, and EDX analysis of AuNPs synthesized from SC. (a) Transmission electron microscopic (TEM) analysis of SC-AuNPs. (b) Scanning electron microscopic (SEM) analysis of SC-AuNPs. (c) Energy dispersive X-ray (EDX) analysis of SC-AuNPs.

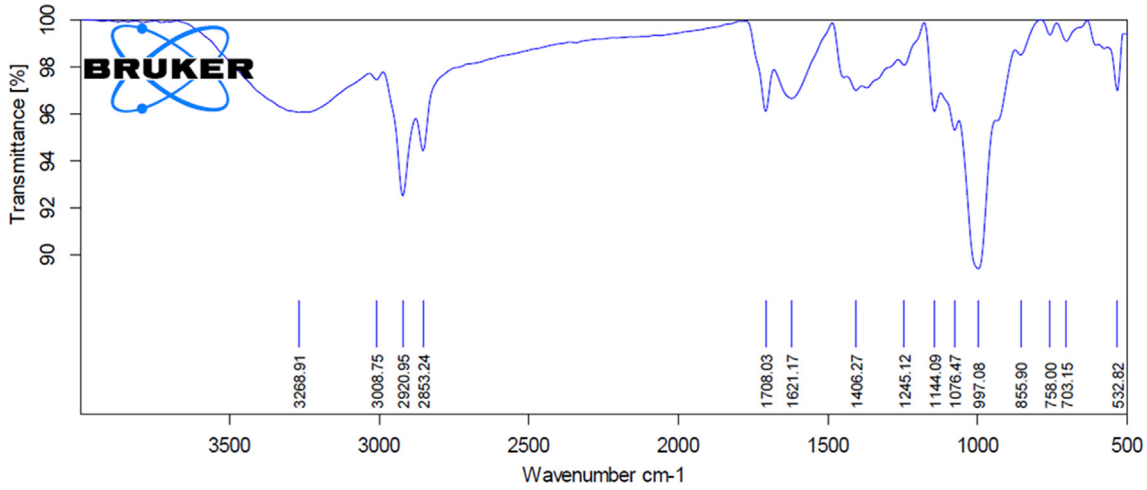

Fig. 4 FTIR analysis of AuNPs synthesized from SC.

Table 1 Effect of AuNPs synthesized from SC on Bodyweight and BMI levels of control and experimental rats.

Groups	Bodyweight (g) (Before experiments)	Bodyweight (g) (After experiments)	BMI (Before experiments)	BMI (After experiments)
Group I	193.42 ± 22.54	194.68 ± 21.36	0.54	0.54
Group II	194.73 ± 51.24*	356.92 ± 34.58*	0.56	1.164
Group III	191.63 ± 74.58*	292.32 ± 28.74*	0.51	0.92
Group IV	193.71 ± 75.95**	280.28 ± 24.29**	0.53	0.76
Group V	192.31 ± 29.43**	255.03 ± 22.31**	0.54	0.65

All data were computed as the mean ± SD of triplicate values (n = 6). The significance level was measured by one-way ANOVA subsequently DMRT test; note: *$p < 0.05$ when compared to the control group and **$p < 0.05$ when compared to the obesity-induced group.

considerable ($p < 0.05$) decrease of the adipose index, leptin, and resistin, whereas, adiponectin increased in comparison to control obese rats as shown in Fig. 5.

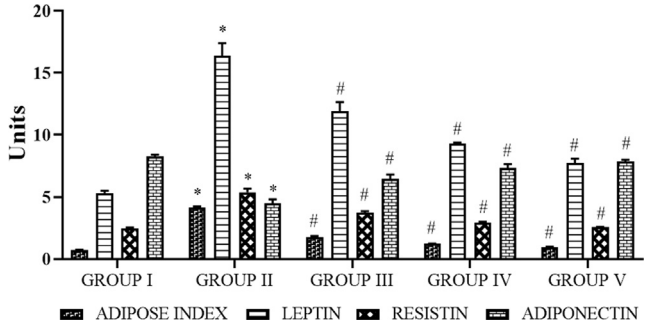

Fig. 5 Photomicrographs show the effects of SC-AuNPs on the adipose index, leptin, resistin, and adiponectin of control, and obese rats. All data were computed as the mean ± SD of triplicate values (n = 6). The significance level was measured by one-way ANOVA subsequently DMRT test; note: *$p < 0.05$ when compared to the control group and #$p < 0.05$ when compared to the obesity-induced group. Group I: Rats fed with the standard pellet food. Group II: Rats fed with HFD and no other treatment. Group III: Rats fed with HFD and 10 mg/kg bwt of SC-AuNPs. Group IV: Rats fed with HFD and 20 mg/kg bwt of SC-AuNPs. Group V: Rats fed with HFD and 30 mg/kg bwt of SC-AuNPs for six weeks by orally.

3.4. Effects of SC-AuNPs on lipid profile

The lipid profile of control and obese animals are shown in Fig. 6. The status of TC, FFA, LDL-C, TG, and VLDL-C was considerably ($p < 0.05$) augmented and the HDL-C was notably ($p < 0.05$) less in HFD treated obese rats when compared to the control rats. The oral supplementation of SC-AuNPs at various concentrations (10, 20 and 30 mg/kg body weight) considerably ($p < 0.05$) reduced the TC, FFA, LDL-C, TG, and VLDL-C levels and notably ($p < 0.05$) augmented the HDL-C level when compared to HFD induced obese rats.

3.5. Effects of SC-AuNPs on coronary risk index (CRI) and atherogenic index (AI)

The AI and CRI of control and obese rats are shown in Fig. 7. The statuses of AI and CRI were considerably ($p < 0.05$) augmented for the HFD treated obese rats when compared to the control animals. Oral supplementation of SC-AuNPs at various concentrations (10, 20, and 30 mg/kg body weight) notably ($p < 0.05$) reduced the CRI and AI levels in comparison to the HFD induced obese rats.

3.6. Effects of SC-AuNPs on liver marker enzymes

The liver marker enzymes of control and obese rats are shown in Fig. 8. The ALP, ALT, and AST status was notably

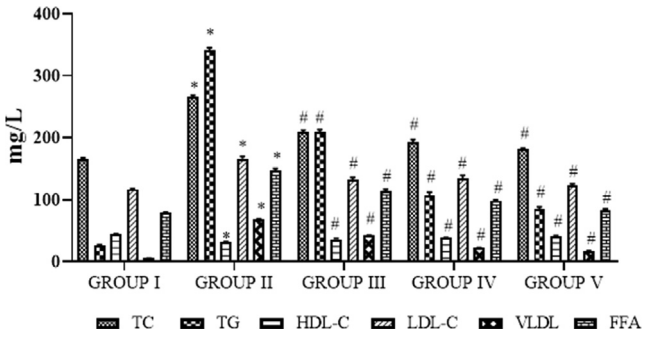

Fig. 6 Photomicrographs show the effects of SC-AuNPs on lipid profile. All data were computed as the mean ± SD of triplicate values (n = 6). The significance level was measured by one-way ANOVA subsequently DMRT test; note: *p < 0.05 when compared to the control group and #p < 0.05 when compared to the obesity-induced group. Group I: Rats fed with the standard pellet food. Group II: Rats fed with HFD and no other treatment. Group III: Rats fed with HFD and 10 mg/kg bwt of SC-AuNPs. Group IV: Rats fed with HFD and 20 mg/kg bwt of SC-AuNPs. Group V: Rats fed with HFD and 30 mg/kg bwt of SC-AuNPs for six weeks by orally.

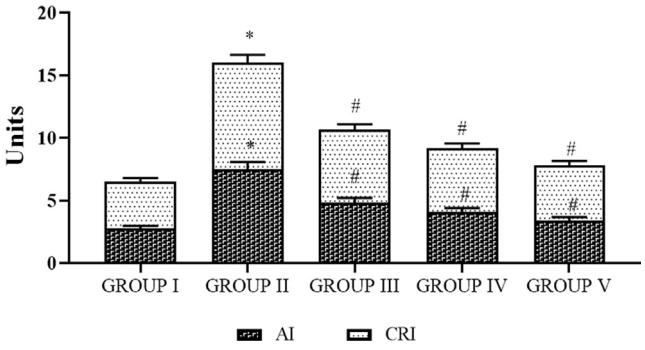

Fig. 7 Photomicrographs show the effects of SC-AuNPs on the atherogenic index (AI) and coronary risk index (CRI). All data were computed as the mean ± SD of triplicate values (n = 6). The significance level was measured by one-way ANOVA subsequently DMRT test; note: *p < 0.05 when compared to the control group and #p < 0.05 when compared to the obesity-induced group. Group I: Rats fed with the standard pellet food. Group II: Rats fed with HFD and no other treatment. Group III: Rats fed with HFD and 10 mg/kg bwt of SC-AuNPs. Group IV: Rats fed with HFD and 20 mg/kg bwt of SC-AuNPs. Group V: Rats fed with HFD and 30 mg/kg bwt of SC-AuNPs for six weeks orally.

(p < 0.05) augmented in the HFD induced obese rats when compared to the control rats. Oral supplementation of SC-AuNPs at various doses (10, 20, and 30 mg/kg body weight) notably (p < 0.05) reduced the liver marker enzymes when compared to the HFD induced obese rats.

3.7. Effects of SC-AuNPs on histopathological changes

Histology evaluation of control animals showed a soft hepatic manifestation lacking any pathological abnormalities as shown in Fig. 9(a). Whereas, in Fig. 9(b), the control obese animals

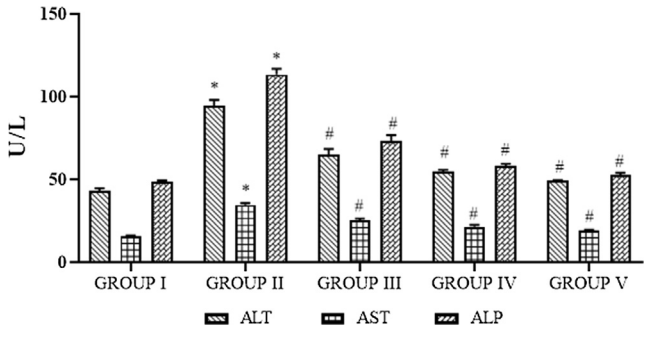

Fig. 8 Photomicrographs show the effects of SC-AuNPs on liver marker enzymes. All data were computed as the mean ± SD of triplicate values (n = 6). The significance level was measured by one-way ANOVA subsequently DMRT test; note: *p < 0.05 when compared to the control group and #p < 0.05 when compared to the obesity-induced group. Group I: Rats fed with the standard pellet food. Group II: Rats fed with HFD and no other treatment. Group III: Rats fed with HFD and 10 mg/kg bwt of SC-AuNPs. Group IV: Rats fed with HFD and 20 mg/kg bwt of SC-AuNPs. Group V: Rats fed with HFD and 30 mg/kg bwt of SC-AuNPs for six weeks orally.

demonstrated deterioration of hepatocytes and increased occurrence of fat cells thus illustrating fat alterations. On the other hand, there were developments in the liver morphology of SC-AuNPs (10, 20, and 30 mg/kg bwt) treated obese rats, where the occurrence of fat cells was not as elevated as those existing in Fig. 9(c)–(e).

3.8. Effects of SC-AuNPs on inflammatory markers

The inflammatory markers of control and obese rats are shown in Fig. 10. The TNF-α and IL-1β levels were notably (p < 0.05) augmented in the HFD treated obese rats when compared to the control animals. Oral supplementation of SC-AuNPs at various doses (10, 20, and 30 mg/kg body weight) considerably (p < 0.05) lowered these inflammatory markers when compared to the HFD induced obese animals.

3.9. Effects of SC-AuNPs on the western blotting protein expression

The pAMPK1α and AMPK1α of control and obese rats are shown in Fig. 11. The levels of AMPK1α were considerably (p < 0.05) augmented and pAMPK1α was notably (p < 0.05) lowered in HFD treated obese rats when compared to the control rats. Oral supplementation of SC-AuNPs at various concentrations (10, 20, and 30 mg/kg body weight) notably (p < 0.05) decreased the level of AMPK1α, while (p < 0.05) augmenting the level of pAMPK1α compared to the HFD induced obese rats.

4. Discussion

Nanoparticles play a significant role in the diverse fields e.g. catalysis, molecular imaging, drug delivery, electrical device, DNA sequencing, and biosensors (Tettey et al., 2012).

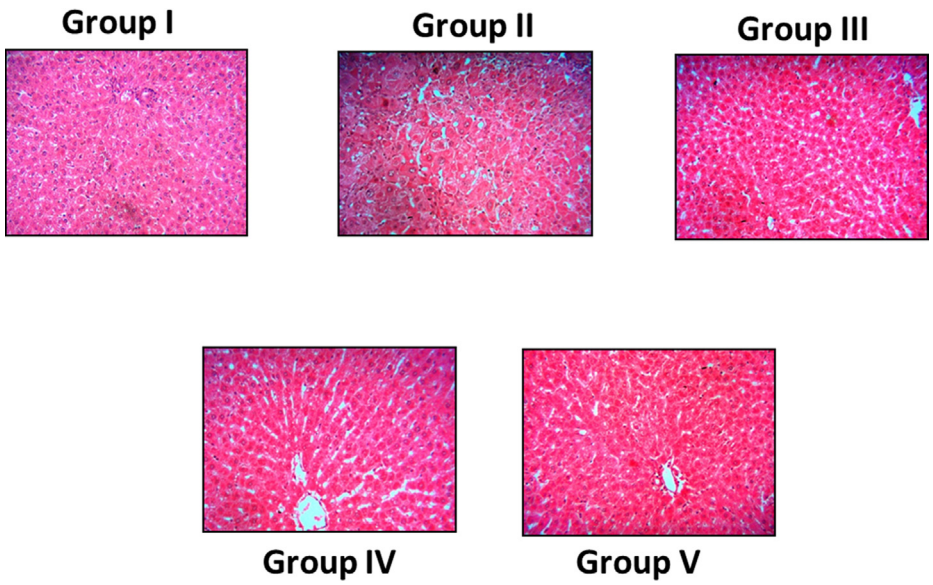

Fig. 9 Photomicrographs show the effects of SC-AuNPs on liver histology of control and obese rats. Groups: (Group I) normal diet rats; (Group II) control obese rats; (Group III) obese rats treated with 10 mg/kg bwt; (Group IV) obese rats treated with 20 mg/kg bwt; (Group V) obese rats treated with 30 mg/kg bwt.

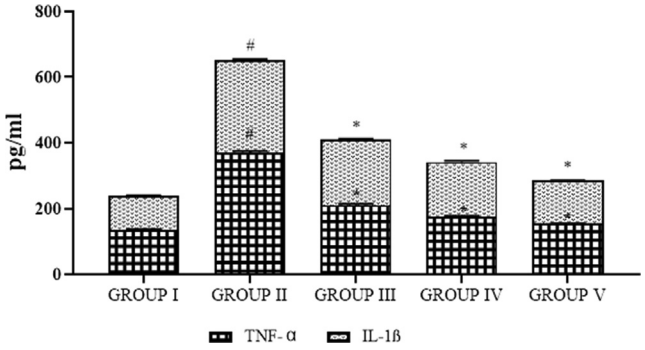

Fig. 10 Photomicrographs show the effects of SC-AuNPs on inflammatory markers. All data were computed as the mean ± SD of triplicate values (n = 6). The significance level was measured by one-way ANOVA subsequently DMRT test; note: $^{\#}p < 0.05$ when compared to the control group and $^{*}p < 0.05$ when compared to the obesity-induced group. Group I: Rats fed with the standard pellet food. Group II: Rats fed with HFD and no other treatment. Group III: Rats fed with HFD and 10 mg/kg bwt of SC-AuNPs. Group IV: Rats fed with HFD and 20 mg/kg bwt of SC-AuNPs. Group V: Rats fed with HFD and 30 mg/kg bwt of SC-AuNPs for six weeks orally.

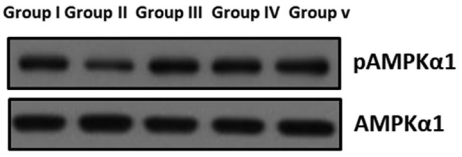

Fig. 11 The effect of SC-AuNPs on AMPK signaling proteins in control and obese rats were examined by western blotting technique. The rats were treated with SC-AuNPs (10, 20, and 30 mg/kg bwt) and the protein expressions of AMPKα1 and pAMPKα1 were determined. β-actin was used as a loading control.

Nanoparticles are extremely essential in the areas of recent sciences involving electronics, chemistry, biology, physics, medicine, and biotechnology. A nanoparticle illustrates exclusive properties that are based on certain features, for example, size, shape, morphology, and scattering (Khan et al., 2016). The utilization of the ideal nano-drug delivery system is decided based on the biochemical and biophysical properties of these nanomaterials for the treatment (Watkins et al., 2015). Nonetheless, the toxicity issues possessed by the nanoparticles cannot be ignored while formulating the nanomedicines. The green route approach of nanoparticles synthesis is extensively promoted as it reduces the toxicity of nanoparticles. Therefore, the use of green nanoparticles for drug delivery can minimize the deleterious effects of drugs (Lam et al., 2017). The UV–visible spectra of synthesized gold nanoparticles were demonstrated by the maximum peak. TEM and SEM analysis confirmed that the particles were spherical and hexagonal in shape and size varying from 20 to 50 nm and EDX spectra established the presence of gold ions. The FTIR assessment of the SC-AuNPs samples established the occurrence of various active groups. The XRD pattern studies demonstrated the existence of nanoparticles with a crystalline structure. Earlier studies also informed that the *Salacia chinensis* is a good source for the production of silver nanoparticles (Jadhav et al., 2015).

The high intake of an HFD can lead to obesity in both animals and humans. Huge amounts of fat accumulate on the adipose tissue and an abnormal lipid metabolism paves the way to obesity (Jung and Choi, 2014). The rats were obese, as the value of BMI was more than normal, which meets the criteria for obesity (Novelli et al., 2007). The therapeutic effects of SC-AuNPs in association with obesity were examined and the risk of obesity was considered. The findings indicated that SC-AuNPs can decrease the extra weight in HFD treated animals

and prevent the risk of liver disease. The determination of the adipose index was computed using the size and number of fat cells that occur in the body's tissues. Liver tissue and skeletal muscle are overloaded with lipids when the defense ability of adipose tissue is damaged (Frayn, 2002). SC-AuNPs treatments significantly decreased the adipose index, leptin, and resistin and increased the adiponectin in HFD induced obese rats. Histopathological evaluation of normal rats showed a smooth hepatic form lacking any pathological abnormalities. The livers of control obese animals demonstrated deterioration of hepatocytes and an augmented occurrence of fat cells illustrating fatty alterations. Conversely, there were developments in the liver morphology of SC-AuNPs administrated obese animals.

The excessive amount of lipid storage in peripheral tissues during obesity might effect in accumulation of excess lipid in the liver and lead to increased hepatic fat levels (Drake et al., 2010). The dyslipidemia is described by distinctive alterations from a lipoprotein profile and normal plasma lipid. Such alterations contain diminished plasma status of HDL with augmented plasma TG and FFA. Those alterations of lipids are generally related to the high production of VLDL, an important structural constituent of these atherogenic lipoproteins; and augmented plasma levels of LDL's (Taskinen, 1995). In our study, notably augmented status of the plasma VLDL-C, TC, FFA, TG, AI, LDL-C, CRI, and reduced HDL-C status was found in HFD induced rats. Previously, the same results were observed in HFD induced mice model (Ezhumalai et al., 2015). Treatment with SC-AuNPs brought these lipid profiles to near normality due to the antilipidemic effect of the SC-AuNPs.

The liver is the essential organ in the process of excretion and metabolism, which regularly carries out the task of biotransformation of environmental pollutants and xenobiotics. AST, ALP, and ALT are the most important liver marker enzymes. The rise of these hepatic marker enzymes on the serum and results of escapes from injured cells reveal the hepatocyte damage. ALT and AST were directly related to the alteration of amino acids to keto acids (Loria et al., 2005). ALP is a membrane-bound glycoprotein, which has been involved in the elevated levels of the sinusoids and the endothelium of the periportal and central veins. It was reported to be implicated in the transfer of metabolites, initiating the protein synthesis, cell membranes, and secretarial functions (Whitehead et al., 1999). Ezhumalai et al. (Ezhumalai et al., 2014; Ezhumalai et al., 2014) reported that HFD induced mice showed increased levels of these liver marker enzymes, concordant with this present investigation. Oral administration of SC-AuNPs in HFD induced obese rats demonstrated a decreased function of these liver marker enzymes.

Adiposity is significantly a dangerous factor for insulin resistance and obesity. Recent data shows the relations between obesity and inflammation (Das, 2001). Inflammatory mediators are produced by adipose tissues that make use of an endocrine effect providing insulin resistance to the liver, vascular endothelial tissue, and skeletal muscle, eventually to the clinical appearance of obesity and type 2 diabetes (Yudkin et al., 1999). Particularly, increased production of adipocyte mediators likes IL-1β and TNF-α, leads to an acute-phase reaction with augmented hepatic formation (Hotamisligil et al., 1995). Improved levels of these inflammatory cytokines were observed in obese rats, whereas, treatment with SC-AuNPs decreased the levels due to the anti-inflammatory effects. AMPK has been recognized as a key controller for the lipid homeostasis, yielding a net result of rising fatty acid oxidation and decreases the production of glycerolipids (Hardie, 2011). The present results indicated that SC-AuNPs significantly decreased the AMPK1α and increased pAMPK1α in HFD induced obese rats. Our results agree with previous results in which pomegranate vinegar has been informed to control the AMPK in HFD induced obese rats (Ok et al., 2013).

5. Conclusion

In this current work, we concluded that the synthesis of SC-AuNPs was characterized. It was principally observed with the ruby red color sample and UV absorption spectra with the highest absorbance. The crystalline nature of SC-AuNPs was verified using XRD. The TEM, SEM, and EDX analyses revealed the size and morphological structures of synthesized nanoparticles. The FTIR results showed the presence of different biomolecules in the SC-AuNPs. Furthermore, SC-AuNPs altered the body weight, BMI, liver marker enzymes, lipid profiles, inflammatory markers, adipose index, leptin, resistin, adiponectin, AI, CRI, AMPKα1, and pAMPKα1 as observed through our experiments.

Declaration of Competing Interest

The authors declare that they have no known competing financial interests or personal relationships that could have appeared to influence the work reported in this paper.

Acknowledgments

This project was supported by Researchers Supporting Project number (RSP-2020/5) King Saud University, Riyadh, Saudi Arabia.

References

Kopelman, P.G., 2000. Obesity as a medical problem. Nature 404, 635–643.

Chen, H., Ng, J.P.M., Tan, Y., McGrath, K., Bishop, D.P., Oliver, B., Chan, Y.L., Cortie, M.B., Milthorpe, B.K., Valenzuela, S.M., 2018. Gold nanoparticles improve metabolic profile of mice fed a high-fat diet. J. Nanobiotechnol. 16, 11.

Brown, M.S., Goldstein, J.L., 1983. Lipoprotein metabolism in the macrophage: implications for cholesterol deposition in atherosclerosis. Annu. Rev. Biochem. 52, 223–261.

Jeevanandam, J., Barhoum, A., Chan, Y.S., Dufresne, A., Danquah, M.K., 2018. Review on nanoparticles and nanostructured materials: history, sources, toxicity and regulations. Beilstein J. Nanotechnol. 9, 1050–1074.

Arvizo, R., Bhattacharya, R., Mukherjee, P., 2010. Gold nanoparticles: opportunities and challenges in nanomedicine. Expert Opin Drug Deliv. 7, 753–763.

Kemp, B.E., Stapleton, D., Campbell, D.J., Chen, Z.P., Murthy, S., Walter, M., Gupta, A., Adams, J.J., Katsis, F., van Denderen, B., Jennings, I.G., Iseli, T., Michell, B.J., Witters, L.A., 2003. AMP-activated protein kinase, super metabolic regulator. BiochemSoc Trans. 31, 162–168.

Kola, B., Grossman, A.B., Korbonits, M., 2008. The role of AMP-activated protein kinase in obesity. Front Horm Res. 36, 198–211.
Benedec, D., Oniga, I., Cuibus, F., Sevastre, B., Stiufiuc, G., Duma, M., Hanganu, D., Iacovita, C., Stiufiuc, R., Lucaciu, C.M., 2018. Origanumvulgare mediated green synthesis of biocompatible gold nanoparticles simultaneously possessing plasmonic, antioxidant and antimicrobial properties. Int. J. Nanomed. 13, 1041–1058.
Chen, H., Ng, J.P.M., Bishop, D.P., Milthorpe, B.K., Valenzuela, S. M., 2018. Gold nanoparticles as cell regulators: beneficial effects of gold nanoparticles on the metabolic profile of mice with pre-existing obesity. J. Nanobiotechnol. 16, 88.
Chen, H., Ng, J.P., Tan, Y., McGrath, K.C., Bishop, D.P., Oliver, B. G., Chan, Y.L., Cortie, M.B., Milthorpe, B.K., Valenzuela, S.M., 2018. Gold nanoparticles improve metabolic profile of mice fed a high-fat diet. J. Nanobiotech., 16
Yi, M.H., Simu, S.Y., Ahn, S., Aceituno, V.C., Wang, C., Mathiyalagan, R., Hurh, J., Batjikh, I., Ali, H., Kim, Y., Kim, S., Yang, D., 2020. Anti-obesity effect of gold nanoparticles from *Dendropanax morbifera* Leveille by suppression of triglyceride synthesis and downregulation of PPARγ and CEBPα signaling pathways in 3T3-L1 mature adipocytes and HepG2 cells. Curr. Nanosci. 16 (2), 196–203.
Deokate, U.A., Khadabadi, S.S., 2012. Phytopharmacological aspects of Salaciachinensis. J. PharmacognosyPhytother. 4, 1–5.
Yoshikawa, M., Pongpiriyadacha, Y., Kishi, A., Kageura, T., Wang, T., Morikawa, T., Matsuda, H., 2003. Biological activities of Salaciachinensis originating in Thailand: the quality evaluation guided by alpha-glucosidase inhibitory activity. YakugakuZasshi 123, 871–880.
Sellamuthu, P.S., Muniappan, B.P., Perumal, S.M., Kandsamy, M., 2009. Antihyerglycemic effect of mengiferin in Streptozotocin induced Diabetic rats. J. Health Sci. 55, 206–214.
Tran, T.M., Nguyen, T.H., Vu, D.T., Tran, V.S., 2008. Study on chemical constituents of Salaciachinensis L. collected in Vietnam. Z. Naturforsch. 141, 1–4.
Asuti, N., 2010. Hepatoprotective activity of ethanolic extract of root bark of Salaciachinensis. J. Pharm. Res. 3, 833–834.
NikNorliza, N.H., Adilah, T.T., Hajar, M.S., Nizam, W.W., Rosli, W. W., 2014. Does extract of pleurotussajor-caju affect liver enzymes and histological integrity?. Ann. Microscopy, 18–27.
Elia, P., Zach, R., Hazan, S., Kolusheva, S., Porat, Z., Zeiri, Y., 2014. Green synthesis of gold nanoparticles using plant extracts as reducing agents. Int. J. Nanomed. 9, 4007–4021.
King, J., 1965. The transferases-alanine and aspartate transaminases. Practical Clin. Enzymol.
Balasubramanian, M.P., Dhandayuthapani, S., Nellaiappan, K., Ramalingam, K., 1983. Comparative studies on phosphomonoesterase in helminths. Helminthologia.
Bergmeyer, H.U., Scheibe, P., Wahlefeld, A.W., 1978. Optimization of methods for aspartate aminotransferase and alanine aminotransferase. Clin. Chem. 24, 58–73.
Lowry, O.H., Rosebrough, M.J., Farr, A.L., Randall, R.J., 1951. Protein measurement with Folin-phenol reagent. J. Biol. Chem. 193, 265–275.
Tettey, C.O., Nagajyothi, P.C., Lee, S.E., Ocloo, A., Minh An, T.N., Sreekanth, T.V., Lee, K.D., 2012. Anti-melanoma, tyrosinase inhibitory and anti-microbial activities of gold nanoparticles synthesized from aqueous leaf extracts of Teraxacumofficinale. Int. J. Cosmet. Sci. 34, 150–154.
Khan, F.A., Zahoor, M., Jalal, A., Rahman, A.U., 2016. Green synthesis of silver nanoparticles by using Ziziphusnummularia leaves aqueous extract and their biological activities. J. Nanomater. 2016, 21.
Watkins, R., Wu, L., Zhang, C., Davis, R.M., Xu, B., 2015. Natural product-based nanomedicine: recent advances and issues. Int. J. Nanomed. 10, 6055–6074.
Lam, P.L., Wong, W.Y., Bian, Z., Chui, C.H., Gambari, R., 2017. Recent advances in green nanoparticulate systems for drug delivery: efficient delivery and safety concern. Nanomedicine (Lond). 12 (4), 357–385.
Jadhav, K., Dhamecha, D., Dalvi, B., Patil, M., 2015. Green synthesis of silver nanoparticles using Salaciachinensis: characterization and its antibacterial activity. ParticulSci. Technol. 33, 445–455.
Jung, U.J., Choi, M.S., 2014. Obesity and its metabolic complications: the role of adipokines and the relationship between obesity, inflammation, insulin resistance, dyslipidemia and nonalcoholic fatty liver disease. Int. J. Mol. Sci. 15, 6184–6223.
Novelli, E.L., Diniz, Y.S., Galhardi, C.M., Ebaid, G.M., Rodrigues, H.G., Mani, F., Fernandes, A.A., Cicogna, A.C., NovelliFilho, J. L., 2007. Anthropometrical parameters and markers of obesity in rats. Lab. Anim. 41, 111–119.
Frayn, K.N., 2002. Adipose tissue as a buffer for daily lipid flux. Diabetologia 45, 1201–1210.
Drake, A.J., Raubenheimer, P.J., Kerrigan, D., McInnes, K.J., Seckl, J.R., Walker, B.R., 2010. Prenatal dexamethasone programs expression of genes in liver and adipose tissue and increased hepatic lipid accumulation but not obesity on a high-fat diet. Endocrinology 151, 1581–1587.
Taskinen, M.R., 1995. Insulin resistance and lipoprotein metabolism. CurrOpinLipidol. 6, 153–160.
Ezhumalai, M., Ashokkumar, N., Pugalendi, K.V., 2015. Combination of carvacrol and rosiglitazone ameliorates high fat diet induced changes in lipids and inflammatory markers in C57BL/6J mice. Biochimie 110, 129–136.
Loria, P., Lonardo, A., Carulli, L., Verrone, A.M., Ricchi, M., Lombardini, S., Rudilosso, A., Ballestri, S., Carulli, N., 2005. Review article: the metabolic syndrome and non-alcoholic fatty liver disease. Aliment PharmacolTher. 22, 31–36.
Whitehead, M.W., Hawkes, N.D., Hainsworth, I., Kingham, J.G., 1999. A prospective study of the causes of notably raised aspartate aminotransferase of liver origin. Gut 45, 129–133.
Ezhumalai, M., Radhiga, T., Pugalendi, K.V., 2014. Antihyperglycemic effect of carvacrol in combination with rosiglitazone in high-fat diet-induced type 2 diabetic C57BL/6J mice. Mol. Cell. Biochem. 385, 23–31.
Das, U.N., 2001. Is obesity an inflammatory condition?. Nutrition 17, 953–966.
Yudkin, J.S., Stehouwer, C.D., Emeis, J.J., Coppack, S.W., 1999. C-reactive protein in healthy subjects: associations with obesity, insulin resistance, and endothelial dysfunction: a potential role for cytokines originating from adipose tissue?. ArterioscIerThrombVasc Biol. 19, 972–978.
Hotamisligil, G.S., Arner, P., Caro, J.F., Atkinson, R.L., Spiegelman, B.M., 1995. Increased adipose tissue expression of tumor necrosis factor-alpha in human obesity and insulin resistance. J. Clin. Invest. 95, 2409–2415.
Hardie, D.G., 2011. Sensing of energy and nutrients by AMP-activated protein kinase. Am. J. ClinNutr. 93, 891S–896S.
Ok, E., Do, G.M., Lim, Y., Park, J.E., Park, Y.J., Kwon, O., 2013. Pomegranate vinegar attenuates adiposity in obese rats through coordinated control of AMPK signaling in the liver and adipose tissue. Lipids Health Dis. 12, 163.